NUMERICAL AERODYNAMIC OPTIMISATION OF 3D HIGH-LIFT CONFIGURATIONS

J. Brezillon, R.P. Dwight, J. Wild
German Aerospace Center
Institute of Aerodynamics and Flow Technology, Braunschweig, Germany

Keywords: ***high-lift, optimisation, evolutionary strategy, adjoint approach, mesh strategy***

Abstract

The paper presents the numerical optimisation activity carried out at DLR for the design of wing-body aircrafts in high-lift configuration. The purpose of the study is to assess the high-fidelity methods and tools needed to optimise the flap and slat settings of 3D configurations in a limited turn-around time. The selected key technologies are successfully applied for the optimisations of 2 different high-lift configurations.

1 Introduction

The wing of an aircraft is classically designed to reach a desired performance at cruise conditions, which is transonic for current commercial aircraft. At landing or take-off, the aerodynamic conditions are so different that such wing cannot fulfil basic requirements without high-lift devices. The aim of such a system is to increase the lift coefficient in order to compensate the low velocity during the take-off and approach phases. Thanks to the deployment of trailing and/or leading edge devices the resulting multi-element wing can reach the necessary aerodynamic performance – typically higher lift – requested for a safe landing and take-off. Nowadays, the demands for noise reduction in the vicinity of the airport have led to stringent regulations that demand efficient and environmental friendly high-lift device design.

Numerical optimisation based on high-fidelity methods is now playing a strategic role in future aircraft design and Computational Fluid Dynamics (CFD) is widely used for the prediction of the aerodynamic performance of the wing, at least in cruise flight. The computation of the flow over a multi-element wing in high-lift configuration remains however one of the most difficult problems encountered in CFD. In Europe, such problems are continuously tackled by various projects funded by the European Commission, in particular the EUROLIFT I and II projects, and flow solvers based on the Reynolds-averaged Navier-Stokes (RANS) equations are able to predict aerodynamic behaviour with good accuracy at reasonable computing cost [1],[2] [3]. However, the wall-clock time required to solve such problems is still too large to include them within a design loop, at least for 3D configurations. At the same time, CFD projects like MEGAFLOW and later MEGADESIGN [4], [5], [6], [7] were initiated within the framework of the German aerospace research program. The main goals of these projects are the development of efficient numerical methods for aerodynamic analysis and optimisation.

As a result of these efforts, this paper presents the numerical optimisation activity carried out at DLR for the optimisation of 3D multi-element aircrafts. Since nowadays the time required by the design process is a key element to capture new market, a challenging time constraint for the 3D optimisation has been set to 2 weeks. The purpose of this study is here to assess the tools and methods needed for the optimisation of a 3D high-lift model within a given (short) wall clock time. After exposing the CFD challenges to simulate an airplane in high-lift configuration, the relevant key technologies to perform the optimisation are presented and then applied on 2 different high-lift configurations.

2 CFD challenges in high-lift design

The aerodynamics around a wing in high-lift configuration is one of the most complex flows occurring around an airplane. Fig. 1 presents an example of the flow field around a wing section of a 3-element wing equipped with a slat at the leading edge and a flap at the trailing edge. Apart the typical boundary layer regions near the walls the multi-element wing presents additional important features like the re-circulation areas in the cut-outs, the mixing of boundary layers and wakes of preceding elements and secondary flows that takes place through the slots between the main wing and high-lift devices. Furthermore, since the high-lift wing operates at high-angle of attack, local supersonic area at the leading edge of the slat and flow separation is most likely to occur on wing and flap upper sides. As a consequence the flow in high lift configuration is dominated by viscous effects. The most appropriate numerical method to correctly capture all these flow features in an acceptable turn around time must be based on compressible Reynolds-averaged Navier-Stokes (RANS) equations.

In order to capture all of these critical flow features a grid of high quality is required. This implies the use of thin cells not only normal to the wall for the accurate discretisation of the boundary layers but also behind the trailing edge of the upstream element and up to the downstream element in order to accurately resolve the wakes until its confluence with the boundary layer of the following elements. A thick layer of thin cells has then to be generated orthogonal to the wall in order to capture the mixing shear layers and the ability of the boundary layer to sustain separation. Furthermore, the high-lift configuration has complicated areas like slots, slat and flap coves, which have to be meshed as well. The selection of the meshing procedure for high-lift design is then a compromise between the flexibility to handle complex configurations, the number of cells for fast computations and the capability to control the space discretisation in particular areas.

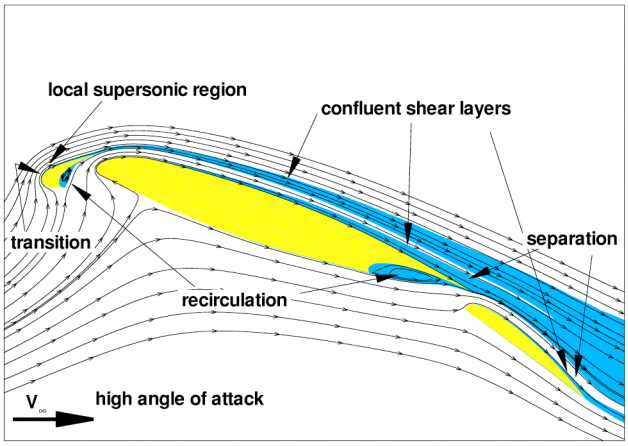

Fig. 1 Flow field around the wing section of a 3-element wing.

A comparison between block-structured and hybrid unstructured approaches for high-lift configurations has already been investigated [8]. On a given - simplified - high-lift configuration and with the same mesh size, the block-structured mesh allows a better stream wise resolution on the leading edges and normal resolution. Additionally a higher cell stretching in spanwise direction is feasible than for hybrid unstructured mesh. However, the hybrid approach clearly simplifies the meshing procedure and permits to consider more complex configurations [9]. A simplification in the structured grid generation process can be achieved with the so-called overset technique, also commonly called chimera technique. This approach has been successfully used for the flow analysis on 3D high-lift configuration [8], [10].

Maintaining a constant mesh quality in high-lift design is a second great challenge as the change of geometry can be rather large. The most relevant design parameters are indeed the relative position of the slat and the flap with respect to the main wing, the so called setting. The shape may also be changed, but since the outer shape of the aircraft is designed for cruise condition, only the shape that is hidden when the devices are retracted is allowed to be modified. In the scope of this paper only the settings of the elements are considered as design parameters. The optimisation of the slot imposes a modification of the mesh surrounding the trailing edge of the preceding elements, which is a critical area in aerodynamics. A change of the

mesh quality in this region can artificially change the flow physics and may slow down the design process or even lead to a non-physical optimum. For all these reasons, the selection of the meshing procedure is driven by its capability to preserve a constant mesh quality during the optimisation process. Various mesh deformation procedures exist and have successfully been used for shape optimisation problems [11], [12] and even for 2D high-lift optimisation [13]. However, this technique applied on large geometric changes can degrade the quality of the resulting mesh due to highly skewed cells. The overset approach seems to be a better strategy since the original mesh is not modified and only cells masked and overlapped are adjusted during the setting optimisation. This approach has been used in 2D high-lift optimisation [14] but the procedure to mask the cells influences the flow around the multi-element wing and can lead to a wrong design [15]. A last approach is to generate new meshes during the optimisation process. If the replay mode of the mesh generator permits to control the mesh properties in almost the complete domain, this procedure will guarantee a sufficiently constant mesh quality during the design. However, the major drawback here is its fastidious setting to get a robust mesh generation process for a large range of setting changes.

3 Ingredients for an efficient optimisation process

3.1 CFD flow solvers

For the resolution of the flow around the high-lift configuration the block-structured FLOWer-Code [16], [17] and the unstructured TAU-Code [18], [19], [20] are available at DLR. Both codes are well established tools for aerodynamic applications in DLR, aerospace industry and universities [5], [21], [22]. Both codes solve the compressible, three-dimensional, unsteady Reynolds-Averaged Navier-Stokes (RANS) equations for rigid bodies in arbitrary motion. For spatial approximation a finite-volume method with second order upwind or central discretization with scalar or matrix artificial dissipation is available. In FLOWer cell centered and cell vertex formulations are provided, whereas TAU uses a vertex centered dual mesh formulation. The discrete equations are integrated explicitly by multistage Runge-Kutta schemes, using local time stepping and multigrid acceleration. In FLOWer the explicit scheme is used in combination with implicit residual smoothing, whereas in TAU the implicit LU-SGS scheme is additionally available. Preconditioning is used for low speed flow simulations. Various turbulence models are available, ranging from eddy viscosity to full differential Reynolds stress models [23] including options for DES (Detached Eddy Simulation). For aerodynamic optimisation, the Spalart-Allmaras model with Edwards modification [24], [25] is preferred for its accuracy and robustness. For a long time only the low Reynolds number formulation has been available in both codes for accuracy reasons, but recently model specific “universal” wall-function have been introduced in the TAU code to achieve a higher efficiency of the solver, especially for use in optimisation. This approach [26] is able to deliver results nearly as good as the low Reynolds number approach for pressure and skin friction distributions over a wide range of y^+ values for the first cell height at the wall, while saving computational time and memory. Both codes can be run in target-lift mode in order to compute the aerodynamic state at a given lift coefficient by automatically adjusting the angle of attack.

Since the efficiency of the flow solver is an important key to reduce the turn around time dedicated strategies have been developed. On multi-block structured meshes, the solver has to handle large vectors and the FLOWer has been accordingly optimised to efficiently run on vector supercomputers like the NEC-SX series. In the same way, a solver based on unstructured mesh has to resolve a single large computational domain that can easily be partitioned in an arbitrary number of domains. Based on domain decomposition and the message passing concept using MPI TAU reaches a high level of efficiency on parallel computers thanks to its optimization for cache processors through

specific edge colouring procedures and load balancing adjusted to the solver needs and the number of requested processors.

Another step forward has been achieved thank to the discrete adjoint solver that was developed within TAU enabling cost-efficient gradient-based aerodynamic optimisation. The advantage of the adjoint method is its ability to evaluate the gradient of a single cost function with respect to a large number of design variables with an effort that scales weakly with the number of design variables [27], [12]. The method consists of the explicit construction of the exact Jacobian of the spatial discretisation with respect to the unknown variables. A wide range of spatial discretisations available in TAU has been differentiated, including the Spalart-Allmaras-Edwards one-equation turbulence model [28], [29]. The effect of various approximations of the Jacobian was first investigated on 2D cases [30] and the efficiency of the adjoint approach has been demonstrated on several 2D and 3D optimisation problems [31], [32]. In the present study, the robustness of the linear solver has been improved for high-lift application by applying the Generalized Minimum Residual (GMRes) method in it's restarted form that requires storage of a given number of Krylov basis function [33].

The metric terms required for the gradient computation are reliably evaluated by finite differences, which imply the necessity of keeping constant the number of grid points while varying the design variables. This process can be done during the CFD run and once the aerodynamic and adjoint states are available, the gradient is extremely fast to compute.

3.2 Meshing procedures

The meshing procedure is a major key component for successfully optimising high-lift configurations, as outline in chapter 2 above. At DLR, large experience has been gained on the set up of mesh for the analysis of complex 3D high-lift configurations [1], [3], [8] as well as 2D optimisations [34], [35]. For aerodynamic analysis, the currently preferred mesh strategy is based on hybrid approach - consisting of prismatic, pyramidal, and tetrahedral elements - generated with the Centaur® software package from CentaurSoft [36]. Well suited for analysis, where the user can iteratively adapt the mesh quality according to his need, this approach turned out to be inefficient in optimisation process since the mesh generation time is long (about hours on complex configurations) and the number of generated mesh points is quite high. For 2D high-lift optimisation, the structured multi-block approach is preferred and reliably executed by MegaCads, an in-house developed system that provides a broad palette of functionalities for CAD and structured mesh generation [37]. However, its application is laborious on 3D high-lift configurations and two alternatives have been investigated. In the first approach, the ICEM-CFD-HEXA tool is employed instead to generate multi-block structured meshes [38]. The software has an interactive part for basic CAD operation, the set-up of the block topology and discretisation, the specification of the boundary conditions and the preparation of the macro to automatically adapt the mesh to a new deformed configuration. The replay file is then latter run in batch modus during the optimisation process. This approach has been applied for the optimisation of the DLR-F11 configuration, a 3D high-lift configuration featuring full span flap and slat - see chapter 4. However, the increasing complexity of the configuration to be designed limits the application of purely structured meshes mainly because of the intricate mesh topology needed.

As a second alternative, a mixed mesh approach has been tested. This relatively new development in mesh generation techniques combines the advantages of structured meshing for the resolution of boundary layers and wakes with the advantages of unstructured mesh generation for its flexibility and cell growing in all 3 dimensions. Pure block structured meshes are employed where the geometry is not too complicated and more topologically difficult areas are meshed with prisms like in the classical hybrid unstructured grid approach. A further step towards quality of these elements has recently been achieved by developing an automatic generator for smooth prismatic layers applying parabolized Laplacian equations [39],

[32]. The rest of the flow field is meshed using tetrahedral elements. This procedure has been implemented in MegaCads by incorporating the 3D triangulation software NETGEN of Schöberl [40] as black box for the generation of the unstructured mesh part. The structured hexahedrons are connected to the unstructured part by collapsing the outer hexahedral layer into prisms and tetrahedrons in order to achieve a smooth transition of the control volumes for the reduction of numerical errors and instabilities. It has already been shown that applying this mesh type can greatly speed up RANS flow computations without losing solution accuracy, mainly due the reduced number of points [41]. This second approach has been selected for the setting optimisation of the FNG configuration that is a 3D high-lift configuration featuring a slat and a flap that does not extend the whole wing span - see chapter 5.

3.3 Optimisation strategies

Optimisation strategies for numerical problems are very well-explored and several hundred algorithms exist, which makes it difficult to test them all to find the most appropriate strategy for 3D high-lift design. We voluntary limit our investigation to three optimization strategies, the Differential Evolution (DE) that belongs to the group of evolutionary algorithms [42]; the gradient free subspace simplex method (SubPlex) [43] and the gradient based sequential quadratic programming algorithm NLPQLP [44], available within modeFRONTIER [45].

These strategies were already evaluated for the design of the shape and position of a 2D flap in high-lift configuration [35]. It has been observed that the evolutionary algorithm is the most robust to failure and uncertainty in the numerical chain, is easily parallelisable and permits to reach the best optimum on multi-modal design space. However, this strategy requires at least one order of magnitude more time to converge than gradient based strategy. On the other hand, the gradient-based strategy is more tedious to use in high-lift configuration since it requires a highly accurate solution with as less uncertainty on the goal function as possible. The gradient free approach obtained the best compromise between efficiency and robustness.

In the present paper, these strategies are tested on the DLR-F11 configuration in order to check their capabilities to efficiently complete the high-lift optimisation problem within 2 weeks.

4 Optimisation of the DLR-F11 configuration

The first configuration optimised is the so called DLR-F11 model with full span flap and slat in take-off configuration. This model is a wide-body Airbus-type research configuration with a half span of 1.4 m that can feature different degrees of complexity [2]. In the present study, six design variables are selected to modify the deflections, the horizontal and the vertical positions of the flap and the slat. The geometric changes are propagated homogenously along the span. The goal is to maximise at a single take-off condition ($Mach$=0.3; Re=20x10^6; AoA=8°) a derived expression of the lift to drag ratio: $Obj = Cl^3 / Cd^2$.

This performance indicator, based on the climb index, has already been successfully employed for flap design based on 2D computations and turned to be better suited than the lift to drag ratio [15]. Additionally, the lift is not allowed to decrease and the angle of attack is kept fix. In order to make a more realistic optimisation the weight of the high-lift system kinematics, which depends on the horizontal deployment capability, is taken into account by penalising the objective function to avoid too heavy a mechanism. The relation between the horizontal displacement and the penalty is set according to industrial specifications [15].

4.1 Parametrisation, mesh procedure and flow solver

Here, an ICEM-CFD macro has been developed to handle both the parametrisation and the mesh procedure. This macro first sets the position of the elements according to the

design variables and computes automatically the flap and slat intersection lines with the body. Once the CAD geometry is ready, the meshing part starts and automatically projects the mesh on the moving part and on the updated intersections lines, sets the position and size of the O blockings surrounding the elements. The resulting structured mesh has in total 2.5 millions points and 25 blocks, see Fig. 2. Four "O" blocks type are designed to discretise the boundary layers, the wakes and to ensure a nominal first cell distance to the wall (y^+=1). The upper part of the main wing is discretised by 73 points to capture the boundary layer and the wake of the slat, see Fig. 3, while 49 points are set for the slot between the main element and the flap. The complete process, from reading the design variables to writing the mesh in either structured or unstructured formats takes about 1 minute on a single AMD Opteron 2.5 GHz processor.

The numerical simulations, either with the FLOWer or the TAU codes, are based on the RANS equations and the Spalart-Allmaras-Edwards turbulence model. For fast convergence, the low Mach number preconditioning approach is adopted and the steady state is reached by a Runge-Kutta scheme using multigrid W-cycles on 3 levels. A fully converged solution with almost 5 orders of density residual decrease is obtained after 1,500 FLOWer or 5,000 TAU cycles. Since the integration scheme to get convergence is differently implemented with more operations for the structured code and since the mesh for TAU computations can be partitioned in an arbitrary number of domains, the total time needed to converge the flow can be almost identical for both codes.

4.2 Optimisations with the FLOWer code

In this first attempt, the numerical flows are computed with the structured FLOWer code, sequentially running on a NEC-SX8. On this computer, which can theoretically reach up to 16 Gflop/s, the flow is fully converged after 2 hours, wall-clock time. This is quite effective and only limited gain is expected by performing parallel computations on this supercomputer.

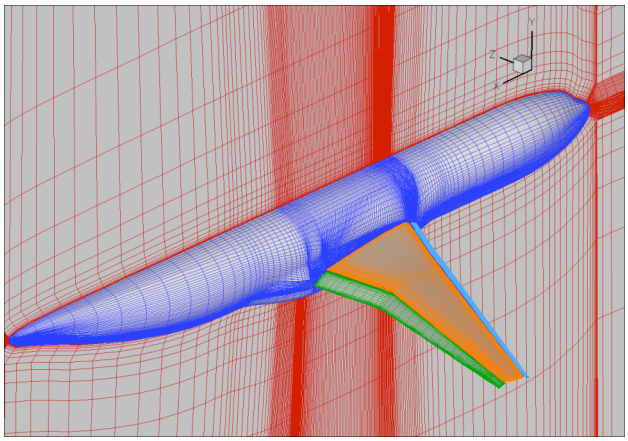

Fig. 2 Multi-block structured mesh around the DLR-F11 model in full span flap and slat configuration.

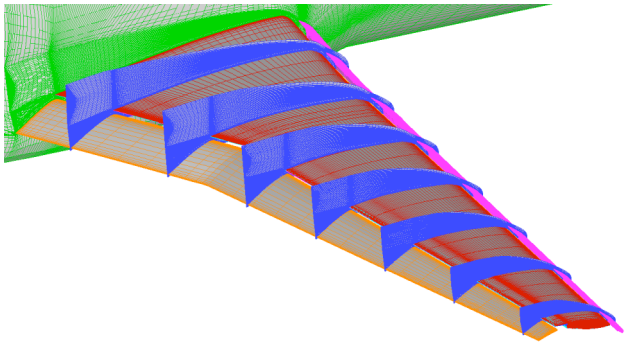

Fig. 3 Close view of the wake discretisation on the top of the DLR-F11 wing.

In order to check the possibility to perform the optimisation within 14 days, three strategies are tested: the DE, the NLPQLP with the gradients evaluated thanks to central finite differences and the SubPlex strategies.

According to previous experiences [35], the DE needs at least 100 generations to converge the population to the optimum. Even on a small population with 10 individuals, the process requires more than 1,000 evaluations. Motivated by the fact that the DE is robust to inaccuracy and easily scalable, it is decided to partially converge the aerodynamic computations and to compute the population in parallel on a cluster. In the present case, a reasonable flow convergence is obtained after 500 iterations and together with a population size set to 10 individuals, the evaluation of a single population on a cluster of 5 NEC-SX8 CPUs is reduced to 1.5 hours, wall-clock time.

In the same way, in order to speed up the optimisation process with the NLPQLP strategy,

the components of the gradients are computed simultaneously. Since the convergence of the optimisation process here depends of the accuracy of the gradients, the aerodynamic computations are fully converged and the gradients are computed with central finite differences: based on a NEC-SX8 cluster with 6 processors, the turn around time for the computation of the gradients is equivalent to only 2 flow computations, i.e. 4 hours, wall-clock time, instead of 24 hours as in a sequential approach.

The SubPlex approach, which involves sequential evaluations only, does not benefit from possible simultaneous computations. A speed up could be obtained by running the FLOWer code in parallel on the NEC, but this was not tested during the study.

Fig. 4 presents the evolutions of the optimisation processes during 14 days, wall-clock time. For the clarity of the figure, only the solutions that fulfill the constraint on the lift level within 0.2% are presented. In order to measure the convergence of the DE algorithm, the best objective and the average objective within one generation are presented. The DE ran up to 162 generations, representing more than 1,600 evaluations, and stopped since the convergence reaches a plateau and the average solution is close to the best optimum. In total the optimisation process required 10 days to converge. The SubPlex algorithm that involves here only one single CPU, presents a convergence rate close to the average solutions from DE. After 14 days and 168 CFD computations, the SubPlex was almost converged and the process was voluntary stopped. On the contrary, the gradient-based strategy was completely converged after 3 days of simulations and 123 evaluations including 108 for the gradients only.

4.3 Optimisations with the TAU code

In a second attempt, the aerodynamic flow is computed with the TAU code running in parallel and the solution is fully converged after 3 hours, wall-clock time, on a cluster of 32 AMD Opteron 2.4 GHz processors.

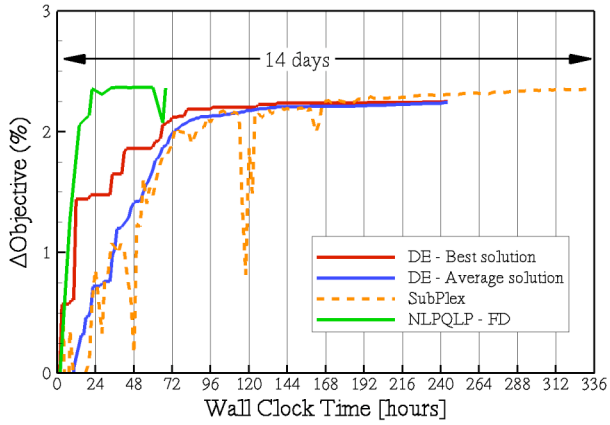

Fig. 4 Objective function according to the wall-clock time - Aerodynamic flows computed with the structured FLOWer code running sequentially on a NEC-SX8.

In order to plenty use the capability of the TAU code, the adjoint mode is here used to efficiently compute the gradients of the lift and drag coefficients. The adjoint states, computed simultaneously on 2 clusters of 16 processors each, the gradients of the objective function and the constraint - derived from the drag and lift gradients - are obtained within 3 hours.

Fig. 5 presents the evolution of the optimisation process obtained with the NLPQLP strategy coupled to the adjoint approach for the computations of the gradients. After 13 evaluations and 78 hours of simulations the optimisation converged to a maximum with a limited deviation on the lift coefficient. Thanks to the adjoint approach, the process is now almost independent to the number of design variables and a more complex optimisation problem involving more design parameters should require almost the same turn around time.

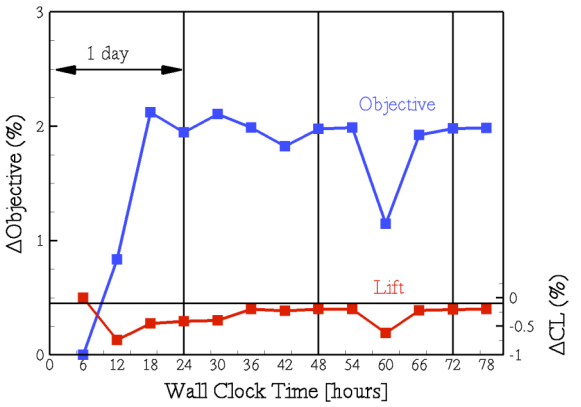

Fig. 5 Objective and lift coefficient according to the wall-clock time - Aerodynamic and adjoint flows computed with the unstructured TAU code.

4.4 Synthesis

All optimisations presented above were obtained within 14 days but with different solvers or levels of convergence. For the sake of comparison, the optimums previously obtained are recomputed with the same flow solver and the same level of convergence and the deviations to the baseline configuration are summarised in Table 1. One can sees that all optimisation strategies give almost the same improvement with a slight advantage of the NLPQLP strategy, independently to the way of computing the gradients. Fig. 6 and Fig. 7 present a comparison of the slat and flap positions at a given spanwise position and confirm that all optimums are located at almost the same position and that both optimums given by the NLPQLP strategy are identical. It can be guessed that the design space is rather shallow close to the optimum and the optimum can be reached only with a fully converged optimisation process, as for the NLPQLP cases.

The performance improvement is made evident by plotting the drag distribution in spanwise direction for each element, see Fig. 8: the optimisation has almost no influence on the drag of the body and the flap but permits to made further negative the drag on the slat. This improvement has to be paid by a lower drag increase on the main wing and the optimised configuration has in total 17.8 counts less drag than on the baseline configuration.

Strategy	ΔObj(%)	ΔCd (dc)	ΔCL(%)
DE	2.2	-16.6	-0.08%
SubPlex	2.3	-17.5	-0.10%
NLPQLP + FD	2.3	-17.8	-0.10%
NLPQLP + Adj.	2.3	-17.8	-0.10%

Table 1 Variations of the objective function, drag (dc=drag count) and lift coefficients.

5 Optimisation of the FNG configuration

The configuration used for the second design case, the so-called FNG wing [46], is similar to the first configuration a wing-body configuration with deployed high-lift devices. The difference to the previous DLR-F11 is that for the FNG the high-lift devices do not extend over the full wing span but are limited to 95% relative span.

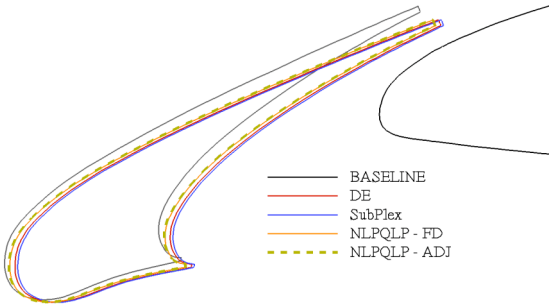

Fig. 6 Slat setting for the baseline and optimised configurations at the middle of the outer wing.

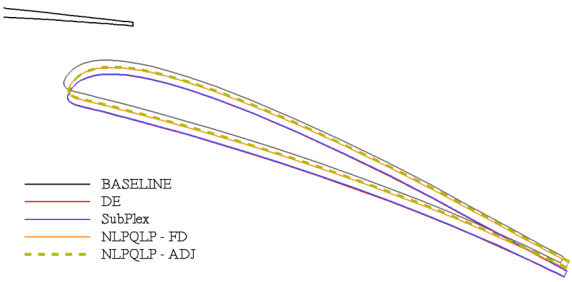

Fig. 7 Flap setting for the baseline and optimised configurations at the middle of the outer wing.

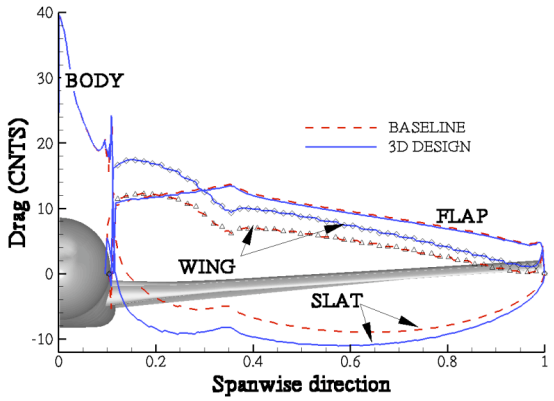

Fig. 8 Drag distribution along the spanwise direction on the baseline and optimised configurations.

By this the topology of the geometry is no longer suited for block structured mesh generation like the DLR-F11 configuration.

The design again is made for a take-off configuration at flight conditions (*Mach*=0.18, Re=18x10^6) and a constant lift coefficient of C_L=1.25. In order to achieve the latter the calculations are all made in target lift mode, where the angle of attack is adapted during the flow calculation. The objective of the optimization is the minimization of drag coefficient. In order to eliminate even smallest deviations of the lift coefficient and its influence on the induced drag, the value used was the actual drag coefficient minus the ideal elliptic induced drag, commonly known as profile drag $C_{Dp} = C_D - C_L^2/\pi\Lambda$.

5.1 Parameterization and meshing procedure

The number of design parameters is increased compared to the previous case by allowing different deflections of the inboard and outboard slat. This reflects that usually for transport aircraft with the engines mounted under the wing the slat is not continuous at the pylon. So there is neither a need nor a restriction for matching slat deflections inboard and outboard the engine. This extends the geometry parameterization to 9 degrees of freedom for the rigid body positioning of the 3 independent devices. As for the DLR-F11 the geometric changes in gap and overlap are propagated at this stage homogenously along the device span.
Since the geometric restrictions at the device ends and their interference with the remaining clean wing tip do not allow for an easy application of block structured meshes, here the mixed mesh type was used. Fig. 9 shows different views of the grid areas meshed with hexahedrons and prisms for the resolution of the viscous flow features, especially boundary layers and wakes. In order to save points for the discretisation of the boundary layer, wall functions were here used. The mesh consists of approximately 2 million grid points, where the number changes only slightly during the optimization in the unstructured part of the grid.

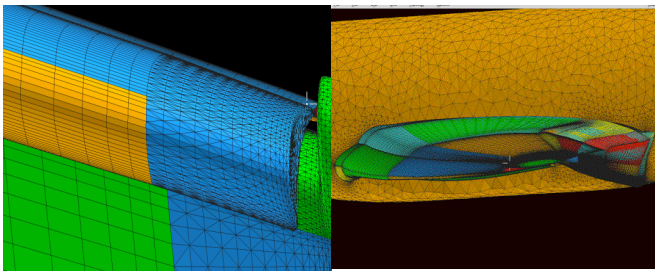

Fig. 9 Views on the outer hull of the structured hexahedral and prismatic areas of the grid around the FNG configuration: (left) detail of grid at slat ending; (right) view on wing and wake areas along wing span.

5.2 Results

For this design only the SubPlex method was applied. The gradient method based on the adjoint could not be applied here due to the variation of the number of grid points in the unstructured mesh part.

The subspace simplex method was run for 5 cycles resulting in overall 150 flow calculations. For the flow calculations 96 processors have been used, resulting in an overall turn-around time of roughly 375 hours or 15 days. The optimum solution has already been found after the third loop, the rest of the optimization secures that there is no better optimum within the range of the parametric changes. Neglecting these iterations would decrease the turn-around time to approximately 11 days.

The objective was reduced by 0.83%, which corresponds to approximately 4 dc. The drag reduction corresponds to a slight gap increase over the whole wing span. The lift coefficient was kept constant within a margin of 0.03%. The relatively small amount of improvement may be explained by the fact that the wing section of the FNG high-lift wing has already been designed applying numerical optimization in 2D and the spanwise variation of the geometry was not included in full extend into the presented exercise.

6 CONCLUSION

The methods and tools developed and successfully applied to perform the settings optimisations of 3D high-lift configurations within a limited time frame were presented. The major key technology to optimise such complex configurations is the meshing procedure and two ways followed at DLR were discussed in detail. The development of efficient and robust numerical methods and the increase of the computer performance permit fast computations of complex flows and makes feasible numerical optimisations within limited turn-around time. It was observed that the evolutionary algorithm is very attractive thanks to his inherent possibility to compute a population in parallel. For strategies involving only sequence of simulations, the reduction of the turn around time can be achieved by conducting CFD in parallel. The gradient-based strategy tested here has permitted to fully converge the optimisation problem within a very short time frame and provides here the best solution. The inclusion of

the adjoint approach gives new opportunities to treat more complex optimisation problems in limited turn around time and will be further investigated at DLR.

References

[1] Thiede P. EUROLIFT - Advanced high lift aerodynamics for transport aircraft. *AIR&SPACE EUROPE*, Vol. 3, No. 3/4, pp. 1-4, 2001.

[2] Rudnik R, Thiede P. European research on high lift commercial aircraft configurations in the EUROLIFT projects. *CEAS/KATnet Conference on Key Aerodynamic Technologies*, Bremen, DE, 2005.

[3] Rudnik R, and Geyr H. The European high lift project EUROLIFT II – Objectives, Approach, and Structure. *25th AIAA Applied Aerodynamics Conference*, AIAA-2007-4296, Miami, FL, 2007

[4] Kroll N, Rossow C-C, Becker K, Thiele F. MEGAFLOW – A numerical flow simulation system. *ICAS 1998 Congress*, Paper 98-2.7.4, Melbourne, Australia, 1998.

[5] Kroll N, Rossow CC, Becker K, Thiele F. The MEGAFLOW project. *Aerospace Science and Technology*, Vol. 4, 2000, pp. 223-237.

[6] Kroll N, Rossow C-C, Schwamborn D, Becker K, Heller G. MEGAFLOW - A numerical flow simulation tool for transport aircraft design. *ICAS 2002 Congress*, Paper 1.10.5, Toronto, Canada, 2002.

[7] Kroll N, Gauger NR, Brezillon J, Becker K and Schulz V. Ongoing activities in shape optimization within the German project MEGADESIGN. *ECCOMAS 2004,* Jyväskylä, Finland, July 2004.

[8] Melber-Wilkending, S, Rudnik R, Ronzheimer A, Schwarz T. Verification of MEGAFLOW-software for high lift applications. *MEGAFLOW - Numerical Flow Simulation for Aircraft Design.* Notes on Numerical Fluid Mechanics and Multidisciplinary Design (NNFM), Vol. 89, pp. 163-178, ISBN 3-540-24383-6, 2005.

[9] Mavriplis DJ, Pirzadeh S. Large-scale parallel unstructured mesh computations for 3D highlift analysis. *37th AIAA Aerospace Sciences Meeting and Exhibit*, AIAA Paper 99-0537, Reno NV, 1999.

[10] Rogers SE, Suhs NE, Dietz WE. PEGASUS 5: An automated pre-Processor for overset-grid CFD. *AIAA Journal*, Vol. 41, No. 6, pp. 1037-1045, 2003

[11] Mavriplis DJ. Multigrid solution of the discrete adjoint for optimization problems on unstructured meshes. *AIAA Journal*, Vol. 44, No. 1, January 2006

[12] Mavriplis DJ. A discrete adjoint-based approach for optimization problems on three-dimensional unstructured meshes. *44th AIAA Aerospace Sciences Meeting and Exhibit*, AIAA Paper 2006-50, Reno NV, January 2006.

[13] Kim S, Alonso JJ, Jameson A. Design optimization of high--lift configurations using a viscous continuous adjoint method. *40th AIAA Aerospace Sciences Meeting and Exhibit*, AIAA Paper 2002-844, Reno NV, January 2002

[14] Moens F. Numerical optimisation of the flap position of a three-element high-lift airfoil in 2d and 2.5d flow using Navier-Stokes solver. *Evolutionary and Deterministic Methods for Design, Optimization, and Control with Applications to Industrial and Societal Problems EUROGEN 2005*, edited by R. Schilling, W. Haase, J. Périaux, H. Baier and G. Bugeda, FLM, ISBN: 3-00-017534-2, Munich, 2005.

[15] Wild J, et al.. Advanced high-lift design by numerical methods and wind tunnel verification within the European project EUROLIFT II. *25th AIAA Applied Aerodynamics Conference,* AIAA-2007-4300, Miami, FL, June 2007

[16] Raddatz J, Fassbender JK. Block structured Navier-Stokes solver FLOWer. *MEGAFLOW - Numerical Flow Simulation for Aircraft Design.* Notes on Numerical Fluid Mechanics and Multidisciplinary Design (NNFM), Vol. 89, pp. 27-44, ISBN 3-540-24383-6, 2005.

[17] Kroll N, Radepiel R, Rossow CC. Accurate and efficient flow solvers for 3D applications on structured meshes. *AGARD R-807*, 4.1-4.59, 1995.

[18] Galle M. Ein Verfahren zur numerischen Simulation kompressibler, reibungsbehafteter Strömungen auf hybriden Netzen. *DLR-FB 99-04*, 1999.

[19] Gerhold T. Overview of the Hybrid RANS TAU-Code. *MEGAFLOW - Numerical Flow Simulation for Aircraft Design.* Notes on Numerical Fluid Mechanics and Multidisciplinary Design (NNFM), Vol. 89, pp. 81-92, ISBN 3-540-24383-6, 2005..

[20] Schwamborn D, Gerhold T, Heinrich R. The DLR TAU-Code: Recent Applications in Research and Industry. *ECCOMAS CDF 2006*, In proceedings of "European Conference on Computational Fluid Dynamics", Delft The Netherland, 2006.

[21] Kroll N, Fassbender JK. MEGAFLOW - Numerical flow simulation for aircraft design. *MEGAFLOW - Numerical Flow Simulation for Aircraft Design.* Notes on Numerical Fluid Mechanics and Multidisciplinary Design (NNFM), Vol. 89, ISBN 3-540-24383-6, 2005.

[22] Kroll N, Rossow CC, Schwamborn D. The MEGAFLOW-project - numerical flow simulation for aircraft. *In A. DiBucchianico, R.M.M. Mattheij, M.A. Peletier (Edts.)*, Progress in Industrial Mathematics at ECMI 2004, Springer, New York, S. 3 – 33, 2005.

[23] Eisfeld B. Numerical simulation of aerodynamic problems with a Reynolds stress model. *In: H.-J. Rath, C. Holze, H.-J. Heinemannm R. Henke, H. Hönlinger (Eds.): New Results in Numerical and Experimental Fluid Mechanics V*, Notes on Numerical Fluid Mechanics and Multidisciplinary Design, Vol. 92, pp. 413-419, 2004

[24] Spalart PR, Allmaras SR. A one-equation turbulence model for aerodynamic flows. *30th AIAA Aerospace Sciences Meeting and Exhibit*, AIAA Paper 92-0439, Reno NV, January 1992.

[25] Edwards J, Chandra S. Comparison of eddy viscosity-transport turbulence models for three-dimensional shock-separated flowfields. *AIAA Journal of Aircrafts*, Vol. 34, No. 4, pp. 756-763, 1996.

[26] Knopp T, Alrutz T, Schwamborn D. A grid and flow adaptive wall-function method for RANS turbulence modelling. *Journal of Computational Physics*, 2006

[27] Jameson A, Martinelli L, Pierce NA. Optimum aerodynamic design using the Navier-Stokes equations. *Theoretical Computational Fluid Dynamics*, Springer, Vol. 10, pp. 213-237, 1998.

[28] Dwight R. Efficiency improvements of RANS-based analysis and optimization using implicit and Adjoint methods on unstructured grids. *School of Mathematics*, University of Manchester, 2006.

[29] Dwight R, Brezillon J, Vollmer D. Efficient algorithms for solution of the adjoint compressible Navier-Stokes equations with applications, *ONERA-DLR Aerospace Symposium (ODAS)*, Toulouse, 2006

[30] Dwight R, Brezillon J. Effect of various approximations of the discrete adjoint on gradient-based optimization. *44th AIAA Aerospace Sciences Meeting and Exhibit*, AIAA Paper 2006-0690, Reno NV, January 2006.

[31] Brezillon J, Dwight R. Discrete adjoint of the Navier-Stokes equations for aerodynamic shape optimisation. *Evolutionary and Deterministic Methods for Design, Optimization, and Control with Applications to Industrial and Societal Problems EUROGEN 2005*, edited by R. Schilling, W. Haase, J. Périaux, H. Baier and G. Bugeda, FLM, ISBN: 3-00-017534-2, Munich, 2005.

[32] Brezillon J, Brodersen O., Dwight R, Ronzheimer A, Wild J. Development and application of a flexible and efficient environment for aerodynamic shape optimisation. *ONERA-DLR Aerospace Symposium (ODAS)*, Toulouse, 2006

[33] Saad Y, Schultz MH. A generalized minimum residual algorithm for solving non-symmetric linear systems. *SIAM Journal of Scientific and Statistical Computing*, Vol. 7, No. 3, pp. 856-859,1988.

[34] Wild J. Validation of numerical optimization of high-lift multi-element airfoils based on Navier-Stokes-equations. *20th AIAA Applied Aerodynamics Conference*, AIAA-2002-2939, St. Louis (USA), 2002.

[35] Brezillon J, Wild J. Evaluation of different optimization strategies for the design of a high-lift flap device. *Evolutionary and Deterministic Methods for Design, Optimization, and Control with Applications to Industrial and Societal Problems EUROGEN 2005*, edited by R. Schilling, W. Haase, J. Périaux, H. Baier and G. Bugeda, FLM, ISBN: 3-00-017534-2, Munich, 2005.

[36] Kallinderis Y. Hybrid grids and their applications. *Handbook of Grid Generation*, edited by J.F. Thompson, B.K. Soni, and N. Weatherill, CRC Press, Boca Raton, FL, 1999, pp. 25.1-25.18.

[37] Brodersen O, Hepperle M, Ronzheimer A, Rossow CC, Schöning B. The parametric grid generation system MegaCads. *Numerical grid generation in computational field simulations*, 5th International Conference, edited by B.K. Soni, Mississippi State Univ, pp. 353-362, 1996.

[38] Ansys, Inc, ICEM-CFD , http://www.icemcfd.com/.

[39] Wild J, Niederdrenk P, Gerhold, T. Marching generation of smooth structured and hybrid meshes based on metric identity. *14th International Meshing Roundtable*, edited by B. Hanks, Springer, Berlin, pp. 109-127, 2005.

[40] Schöberl J. NETGEN - An advancing front 2D/3D mesh generator based on abstract rules. *Computing and Visualization in Science*, Vol. 1, pp. 41-52, 1997.

[41] Wild J. Acceleration of aerodynamic optimization based on RANS-Equations by using semi-structured grids. *ERCOFTAC Design Optimization: Methods & Applications*, Paper ERCODO2004_221, Athens (Greece), 2004

[42] Storn R, Price K. Differential Evolution - a simple and efficient adaptive scheme for global optimization over continuous spaces. *Technical Report*, International Computer Science Institute, TR-95-012, Berkley, 1995.

[43] Rowan T. Functional stability analysis of numerical algorithms, *Thesis*, Department of Computer Sciences, University of Texas at Austin, USA 1990.

[44] Schittkowski K. NLPQLP: A new Fortran implementation of a sequential quadratic programming algorithm for parallel computing. *Report*, Department of Mathematics, University of Bayreuth, 2001.

[45] Esteco, modeFRONTIER v4, http://www.esteco.com/

[46] Dargel, G., Hansen, H., Wild, J., Streit, T., Rosemann, H. Aerodynamische flügelauslegung mit multifunktionalen steuerflächen (aerodynamic design of wings with multi-functional control devices). *DGLR Jahrbuch 2002*, DGLR-2002-096, Vol I, DGLR, (2002), pp. 1605

Copyright Statement